

CBPF-NF-011/89

FISSION OF Al, Ti, Co, Zr, Nb, Ag, In, Nd, Sm, AND Ta  
NUCLEI INDUCED BY 0.8-1.8 GeV PHOTONS

by

D.A. de LIMA\*<sup>†</sup>, J.B. MARTINS<sup>1</sup> and O.A.P. TAVARES<sup>1</sup>

<sup>1</sup>Centro Brasileiro de Pesquisas Físicas - CBPF/CNPq  
Rua Dr. Xavier Sigaud, 150  
22290 - Rio de Janeiro, RJ - Brasil

\*Departamento de Física  
Universidade Federal da Paraíba  
58000 - João Pessoa, PB - Brasil

<sup>†</sup>Present address: Istituto Nazionale di Fisica Nucleare,  
Laboratori Nazionali di Frascati, Frascati (Roma), Italia.

ABSTRACT—Samples of Al, Ti, Co, Zr, Nb, Ag, In, Nd, Sm, and Ta elements in contact with solid state nuclear track detectors were exposed to 0.8-1.8 GeV bremsstrahlung beams at the 2.5-GeV Electron Synchrotron of the Bonn University. The detectors were processed to produce visible fission tracks for track analysis with optical microscopes. Absolute mean cross section per photon and fissility were evaluated. Results are discussed and compared with other photofission data as well as with estimates from the current fission models. A broad minimum found for nuclear fissility of  $10^{-4}$ - $10^{-3}$  covering the range  $15 \lesssim Z^2/A \lesssim 25$  seems to confirm the predictions from the models. For Al and Ti nuclei the probability of fission amounts to  $\sim 10^{-1}$ .

Key-words: Photofission cross-section; Nuclear fissility; Bremsstrahlung; 0.8-1.8 GeV; Medium-weight nuclei; Plastic track detectors.

## 1. - Introduction

Fission cross section measurements of light and intermediate-mass nuclei are at present still scanty, particularly for the case of fission induced by intermediate-energy photons as incident particles. Photofission experiments of complex nuclei of  $A \leq 180$  have been carried out by using nuclear-track detectors, either etchable solid state detectors (1-5) or nuclear emulsion (6). In spite of difficulties encountered during experiments the available photofission data are of good quality, although in some cases disagreement there still exists, specially in the region of target nuclei located around silver.

From the theoretical point of view, estimates of nuclear fissility (probability of fission) by Nix and Sassi (7) and Il'inov et al. (8) have indicated a broad minimum in the curves fissility versus  $Z^2/A$  ( $Z$  and  $A$  denoting, respectively, atomic and mass numbers) covering the range  $15 \leq Z^2/A \leq 25$ , i.e., the region of intermediate-mass nuclei extending approximately from As up to Sm. Since the current fission models (9) have predicted a maximum value in the fission barrier for nuclei around silver, and to compare new fissility data with predictions, we decided, therefore, to conduct a series of fission experiments aiming at determine cross section and fissility induced by intermediate-energy photons for a number of target nuclei in the range  $6 \leq Z^2/A \leq 30$ .

In recent years, the development of new solid state nuclear track detection methods (10), particularly the use of CR-39 track detectors in several branches of nuclear science (11), has opened new possibilities of obtaining particle-induced fission

cross section data of nuclei lighter than Co.

The purpose of the present work is contribute to new fissility data by investigating fission of Al, Ti, Co, Zr, Nb, Ag, In, Nd, Sm, and Ta nuclei induced by bremsstrahlung of maximum energy in the range 0.8-1.8 GeV. Results are compared with data from other laboratories and estimated values of nuclear fissility taken from literature as well. Preliminary results of the experiment described in the present paper have been already published elsewhere in summary form only (12,13).

## 2. - Experimental

The experiment consisted firstly of stacking thick metal foils of Co, Zr, Nb, Ag, In, and Ta target elements each facing a 100- $\mu$ m thick makrofol polycarbonate track detector. Similarly, Al and Ti target elements were placed in contact with plates of  $\sim$  1 mm thick CR-39 polymer track detectors. It was prepared also thin films of Nd and Sm target elements on muscovite mica sheets as track detector. All these materials were kept close together by enclosing it between two sheets of a heat-sealable plastics and them vacuum packed.

The stacks were exposed perpendicularly to high-intensity bremsstrahlung beams of 0.8, 1.0, 1.4, and 1.8 GeV end-point energies at the Bonn 2.5-GeV Electron Synchrotron with typical total number of photons in the range  $10^{12}$ - $10^{14}$  equivalent quanta/cm<sup>2</sup> measured by a quantameter.

In order to make fission tracks visible for track analysis under optical microscopy the CR-39 plates were

submitted later to a 6.25 N NaOH etching at 60°C during two or three periods of 1 h each without stirring. Under these conditions, a bulk etch rate  $V_G = 0.5 \pm 0.1 \mu\text{m/h}$  was obtained by measuring the thickness of material removed by etching with time. In the case of makrofol sheets an identical etching solution was used, this time at 70°C during three periods of 20 min each. By the same method as for CR-39 plates, a bulk etch rate  $V_G = 1.9 \pm 0.1 \mu\text{m/h}$  was obtained. For mica detectors, after removing of the Nd and Sm films, they were submitted to an etching procedure consisting of 40% hydrofluoric acid at 23°C during 2h.

The scanning of the detector surfaces and measurements of the geometrical quantities of etched tracks were carried out by using Leitz Ortholux microscopes fitted out with oculars of 15× with calibrated eye-pieces, and dry objectives of 45× magnification. The use of thick samples in contact with track detectors of different sensitivities made it necessary to solve new problems in order to obtain the final photofission yields <sup>(14)</sup>. The scanning procedure consisted of careful measurements of the scanning areas, track-lengths, dip-angles, and the evaluation of counting efficiency.

### 3. - Photofission Yields

Whenever thick samples are used in contact with track detectors it becomes necessary to know the number of target nuclei of the sample which actually contributes to fission events recorded. For this purpose we developed a method which has been

described in details in Ref. (14), from which the photofission yield,  $\sigma_Q$ , can be obtained by

$$(1) \quad \sigma_Q = \frac{1.15 N_T}{Q \frac{\rho N_0}{M} \frac{\bar{a}_0}{2} \left(1 - \frac{r_m}{\bar{r}_0}\right) \cos^2 \bar{\phi}_c}$$

In this expression,  $N_T$  is the total number of fission tracks observed per unit area,  $Q$  is the number of equivalent photons incident on the target-detector stack per unit area,  $\rho$  is the density of the sample material ( $\text{g/cm}^3$ ),  $N_0$  is Avogadro's number,  $M$  is the atomic weight,  $\bar{a}_0$  and  $\bar{r}_0$  are the average full residual ranges of fission fragments, respectively, in the sample and detector,  $r_m$  is the minimal etched track length in the detector measured under the optical system used, and  $\bar{\phi}$  is the average critical angle of track etching (measured from the detector surface). The factor 1.15 corrects the number of tracks observed for losses due to identification of tracks near track-length threshold. In equation (1), we identify and interpret the quantity  $\bar{a}_0/2$  as the average effective thickness of a thick target, the quantity  $1 - r_m/\bar{r}_0$  as the average efficiency factor related to observation of tracks, and  $\cos^2 \bar{\phi}_c$  as the average etching efficiency. Formula (1) above has been used to obtain the photofission yields for Al, Ti, Co, Zr, Nb, Ag, In, Nd, and Ta thick target elements.

To obtain the values of  $\bar{a}_0$ , firstly we calculated the mean incident photon energy,  $\bar{k}$ , in the bremsstrahlung spectrum (assumed of the form  $1/k$ ) from photofission threshold up to end-point energy. The photofission thresholds were estimated based on the work of Methasiri and Johansson (1). For each

irradiation condition, i.e., target element plus mean photon incident energy, and by assuming the symmetrical mode of fission, the atomic number,  $Z_f$ , and the mass number  $A_f$  of a typical fission fragment was obtained by

$$(2) \quad Z_f = \frac{Z}{2} - \frac{\Delta z + \Delta Z}{4}$$

$$(3) \quad A_f = \frac{A}{2} - \frac{\Delta z + \Delta n + \Delta A}{4} ,$$

where  $Z$  and  $A$  represent, respectively, the atomic number and mass number of the target nucleus,  $\Delta z$  and  $\Delta n$  denote, respectively, the number of protons and neutrons lost during the intranuclear cascade which follows the absorption of a high-energy incident photon by the nucleus, and  $\Delta Z$  and  $\Delta A$  represent, respectively, the total number of protons and nucleons lost by the target nucleus after nuclear photointeraction. Values for the quantities  $\Delta z$ ,  $\Delta n$ ,  $\Delta Z$ , and  $\Delta A$  were obtained based on the work by Barashenkov et al. (15). For each typical fission fragment, we constructed range-energy curves for both detector and target materials according to routine calculation developed by Andersen and Ziegler (16). Hence, the kinetic energy of a typical fragment was obtained from the first range-energy curve and, finally, the value of  $\bar{a}_0$  was evaluated by using the second range-energy curve. The evaluation of the quantity  $\bar{r}_0$  has been done as described in Ref. (14).

In the case of Sm thin targets, the yields were obtained by the usual formula

$$(4) \quad \sigma_Q = \frac{N_T}{Q \frac{\rho N_0}{M} x (1 - \sin \bar{\phi}_c)}$$

where  $x$  is the thickness of the target sample, and  $1 - \sin \bar{\phi}_c$  is the etching efficiency.

The photofission yields which were obtained as described above (expressed as cross section per equivalent quantum) are presented in Table 1 (last column). The errors indicated are statistical ones, and they represent a combination of the errors associated to all quantities needed for the evaluation of the cross section. In the case of Nd target, measurements carried out by using mica as detector have given yield values systematically greater than those obtained by making use of makrofol. This might be caused by some systematic errors the origin of which was not easy to identify.

#### 4. - Absolute Mean Photofission Cross Section and Fissility

In bremsstrahlung-induced reactions the measured yields,  $\sigma_Q$ , represent the sum of the contributions to a particular type of event due to photons of the bremsstrahlung spectrum with energies  $k$  from threshold to maximum energy  $E_0$ . If use is made of the common  $1/k$  spectrum approximation for the different high-energy bremsstrahlung of end-point energy  $E_0$ , the absolute cross section per photon within a small  $E_0$  energy-range can be calculated by the usual formula

$$(5) \quad \sigma = \frac{d\sigma_Q}{d(\ln E_0)}$$



Therefore, the photofission cross section for a given target element is given by the slope of the curve  $\sigma_Q$  versus  $\ln E_0$ . In figures 1 and 2 we plotted the yield-values for the different irradiation conditions as a function of  $\ln E_0$ . In each case, a linear dependence was assumed since we have only few measured yields. By using least-squares analysis, and rejecting the disaligned points, the value of the mean absolute photofission cross sections in the range 0.8-1.8 GeV were derived (Table 2, column two).

Next, the mean nuclear fissility values have been obtained by calculating the ratio  $f = \bar{\sigma}_f / \bar{\sigma}_t$  of mean photofission cross section to mean total nuclear photoabsorption cross section. In the energy range considered (0.8-1.8 GeV),  $\bar{\sigma}_t$  was evaluated by the expression

$$(6) \quad \bar{\sigma}_t = A \bar{\sigma}_{\gamma N} \delta \approx 180A \text{ } \mu\text{b} \quad ,$$

where A denotes mass number,  $\bar{\sigma}_{\gamma N}$  is the mean total nucleon photoabsorption cross section (<sup>17</sup>), and  $\delta$  is a factor which corrects for screening effects caused by the nuclear surface (<sup>18,19</sup>). As usual, values of  $\bar{\sigma}_{\gamma N}$  have been corrected for nucleon motion. Nuclear fissility values for the different nuclei studied in the present work are listed in Table 2 (column five). It is seen that for Al and Ti target nuclei the fissility amounts to about 0.1, whereas for the other nuclei it is within the range  $3 \times 10^{-4} - 3 \times 10^{-3}$ .

## 5. - Comparison with other Photofission Data and Conclusions

A comparative study of the results of the present work with other experimental photofission data taken from literature is presented in Fig. 3, where we plotted fissility values as a function of  $Z^2/A$  of the target nucleus. Most data show reasonable agreement between each other, although in some cases they differ by 1-2 orders of magnitude. Some estimated values of nuclear fissility (Monte Carlo calculations) based on the cascade-evaporation model for high-energy photonuclear reactions and the liquid-drop model for fission by Il'inov et al. (8) for 600-MeV monoenergetic photons, as well as estimates by Nix and Sassi (7) based on an evaporation-fission-competition process, are also reported to allow a comparison. All data seems to confirm the existence of a broad minimum covering the region of intermediate-mass nuclei as predicted by the above mentioned current models. Of course, a number of new, additional experimental data are required to allow for a more refined analysis, specially in the region of light nuclei.

The authors wish to express their gratitude to Dr. D. Husmann for the opportunity and interest in exposing the target-detector systems. The assistance by the technical machine staff of the 2.5-GeV Elektronen Synchrotron of the Universität Bonn during irradiations is gratefully acknowledged. Discussions with E.L. Medeiros were very stimulating and greatly appreciated. D.A. de Lima thanks the Centro Brasileiro de Pesquisas Físicas-CBPF/CNPq for the warm hospitality he received during development of this work. The partial support by the Brazilian CNPq, CAPES, and CNEN is also gratefully acknowledged.

Figure Captions

Fig. 1 - Photofission yields, expressed as cross section per equivalent quantum ( $\sigma_0$ ), plotted against bremsstrahlung energy  $E_0$  (log scale). Points represent results of measurements obtained in the present experiment for target-detector combinations as indicated. The straight lines are least-squares fits to the points.

Fig. 2 - Same as in figure 1.

Fig. 3 - Nuclear fissility versus  $Z^2/A$  of some selected photon-induced fission experiments. Data are as follows:  $\nabla$ , glass detector, 0.3-0.9 GeV, ref. (1);  $\circ$ , glass detector, 1-6 GeV, ref. (20);  $\Delta$ , glass detector, 1-6 GeV, ref. (21);  $\square$ , nuclear emulsion, 1-6 GeV, ref. (22);  $\nabla$ , glass detector, threshold-1 GeV, ref. (3);  $\diamond$ , mica detector, threshold-1 GeV, ref. (5);  $\blacklozenge$ , glass detector, threshold-1.6 GeV, ref. (23);  $\dagger$ , nuclear emulsion, 1-6 GeV, ref. (6);  $\bullet$ , glass detector, 0.6-1.5 GeV, ref. (2);  $\blacksquare$ , glass and mica detectors, 580 MeV, ref. (4);  $\blacksquare$ , CR-39 detector, 0.8-1.8 GeV, this work;  $\bullet$ , makrofol detector, 0.8-1.8 GeV, this work;  $\blacktriangle$ , mica detector, 0.8-1.8 GeV, this work. Theoretical estimates (Monte Carlo calculations) are represented by lines: ----, curve VI of ref. (7); --, 600-MeV monoenergetic photons assuming a level density parameter  $a = 0.10 \text{ MeV}^{-1}$  with shell effects included of ref. (8); —, 600-MeV monoenergetic photons assuming  $a = 0.05 \text{ MeV}^{-1}$  of ref. (8).

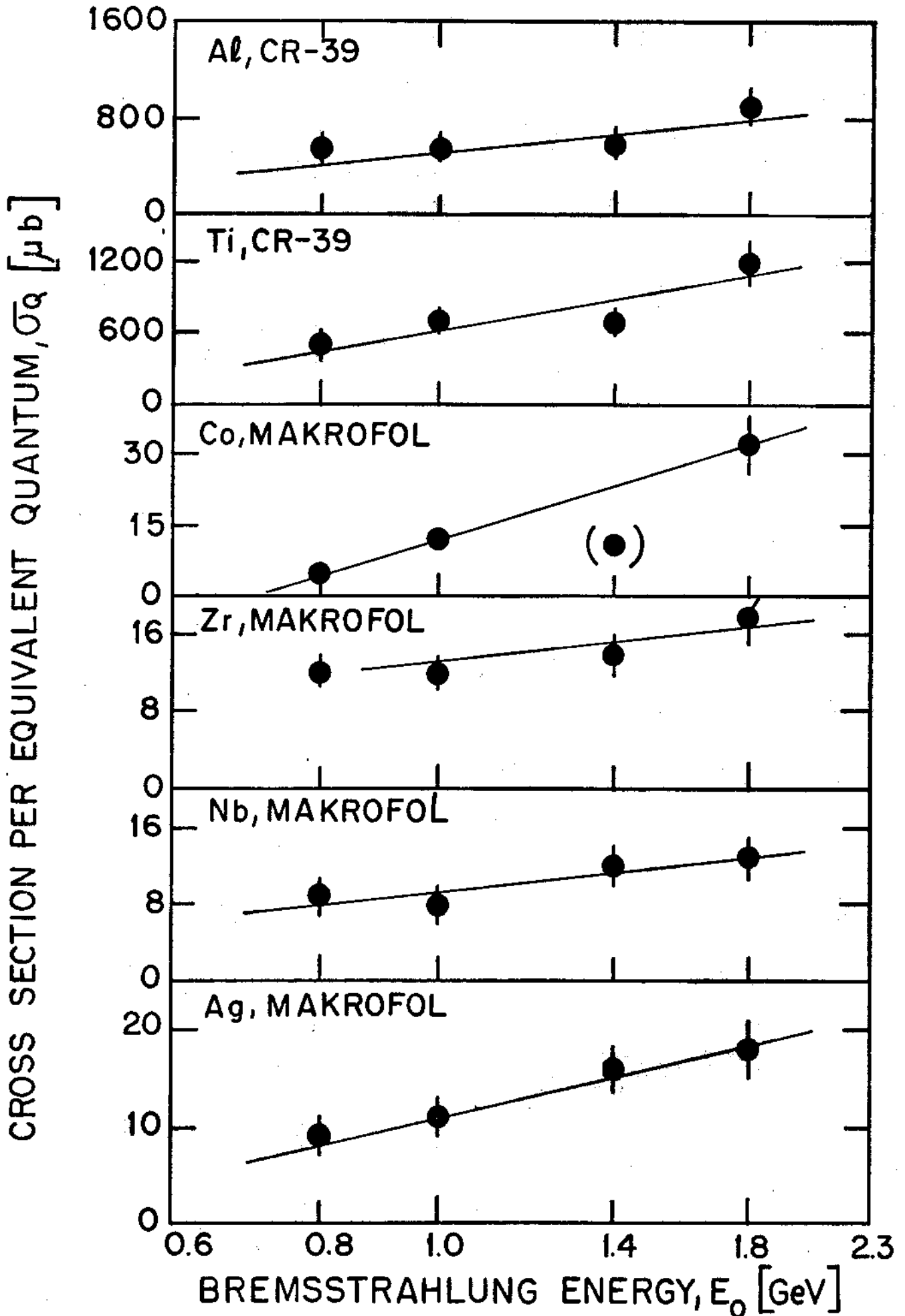


Fig. 1

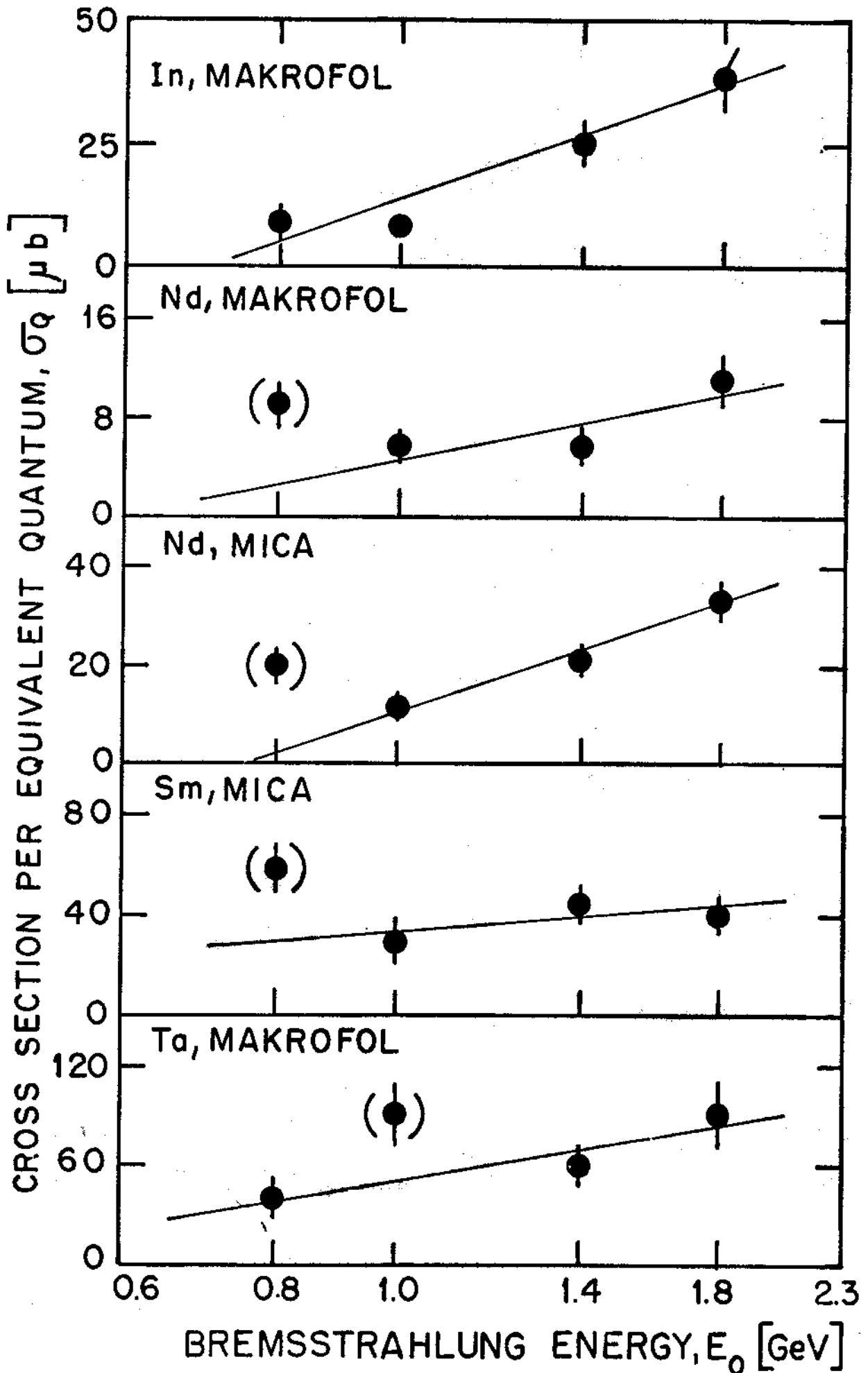


Fig. 2

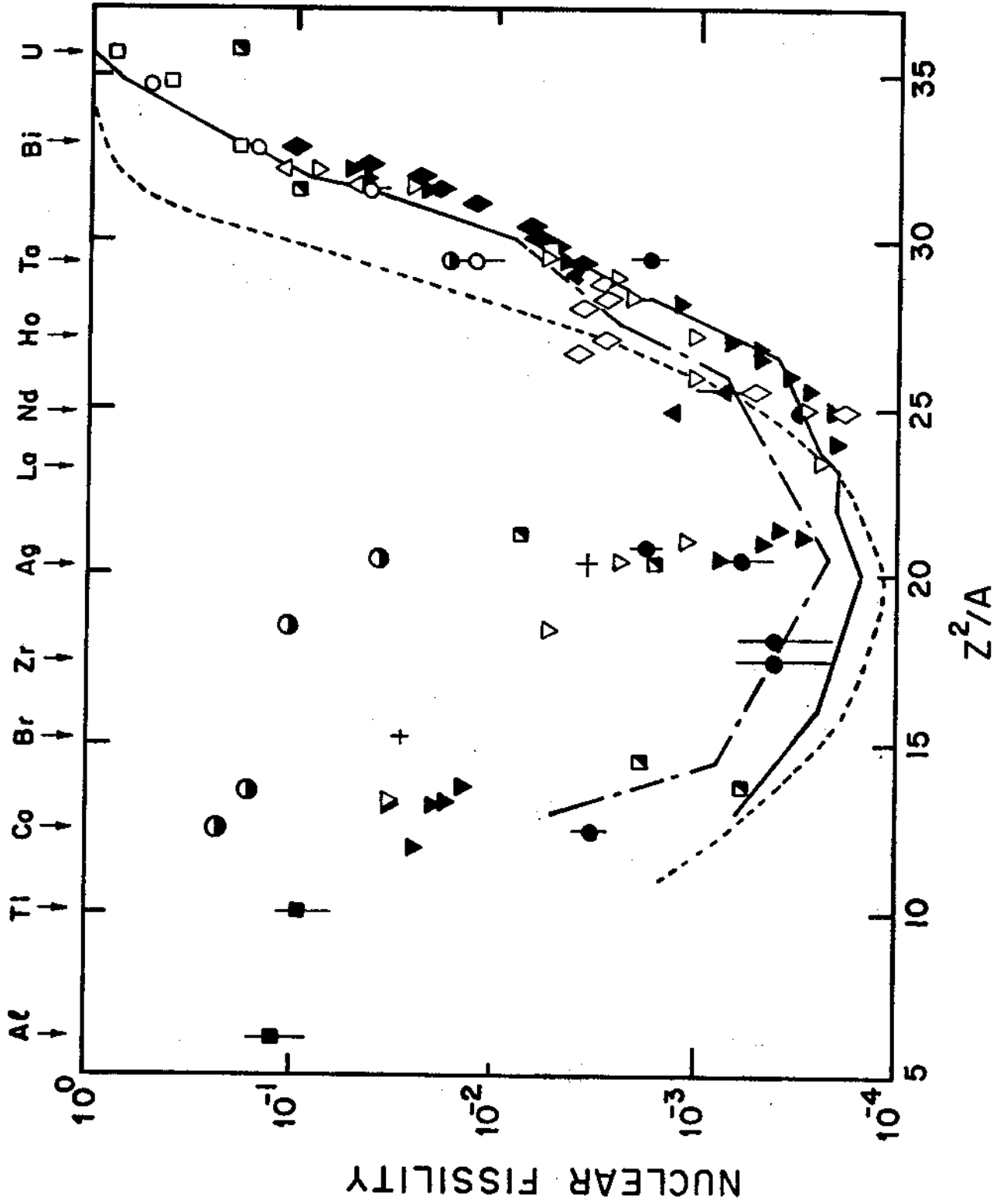


Fig. 3

Table 1 - Data regarding the determination of the photofission yields.

Target nucleus and detector	Effective number of target nuclei [ $10^{18} \text{ cm}^{-2}$ ]	Bremsstrahlung maximum energy $E_0$ [GeV]	Number of equivalent quanta $Q$ [ $10^{12} \text{ cm}^{-2}$ ]	Number of fission tracks per unit area $N_T$ [ $10^3 \text{ cm}^{-2}$ ]	Total efficiency factor	Photofission yield $\sigma_Q$ [ $\mu\text{b}$ ]
Al CR-39	22	0.8	1.0	1.2	0.10	$(5.6 \pm 0.9) \times 10^2$
	22	1.0	1.0	1.2	0.10	$(5.5 \pm 0.9) \times 10^2$
	22	1.4	1.0	1.3	0.10	$(6 \pm 1) \times 10^2$
	22	1.8	1.0	2.0	0.10	$(9 \pm 1) \times 10^2$
Ti CR-39	15	0.8	1.0	0.74	0.10	$(4.9 \pm 0.9) \times 10^2$
	15	1.0	1.0	1.1	0.10	$(7 \pm 1) \times 10^2$
	15	1.4	1.0	1.1	0.10	$(7 \pm 1) \times 10^2$
	15	1.8	1.0	1.8	0.10	$(12 \pm 2) \times 10^2$
Co Makrofol	14	0.8	28.4	0.67	0.35	$4.8 \pm 0.9$
	14	1.0	29.6	1.7	0.35	$12 \pm 2$
	14	1.4	30.0	1.6	0.35	$11 \pm 2$
	14	1.8	30.0	4.7	0.35	$32 \pm 6$
Zr Makrofol	8.2	0.8	28.4	0.89	0.32	$12 \pm 2$
	8.2	1.0	29.6	0.93	0.32	$12 \pm 2$
	8.2	1.4	30.0	1.1	0.32	$14 \pm 3$
	8.2	1.8	30.0	1.4	0.32	$18 \pm 3$
Nb Makrofol	9.2	0.8	28.4	1.0	0.43	$9 \pm 2$
	9.2	1.0	29.6	0.94	0.43	$8 \pm 2$
	9.2	1.4	30.0	1.4	0.43	$12 \pm 2$
	9.2	1.8	30.0	1.5	0.43	$13 \pm 3$
Ag Makrofol	11	0.8	28.4	1.2	0.42	$9 \pm 2$
	11	1.0	29.6	1.5	0.42	$11 \pm 2$
	11	1.4	30.0	2.2	0.42	$16 \pm 3$
	11	1.8	30.0	2.5	0.42	$18 \pm 3$
In Makrofol	9.8	0.8	28.4	1.0	0.40	$9 \pm 2$
	9.8	1.0	29.6	0.93	0.40	$8 \pm 2$
	9.8	1.4	30.0	2.9	0.40	$25 \pm 5$
	9.8	1.8	30.0	4.5	0.40	$38 \pm 7$
Nd Makrofol	7.7	0.8	28.4	1.0	0.55	$9 \pm 2$
	7.5	1.0	29.6	0.66	0.55	$5.4 \pm 0.9$
	7.2	1.4	30.0	0.67	0.55	$5.7 \pm 0.9$
	5.1	1.8	30.0	0.93	0.55	$11 \pm 2$
Nd Mica	5.1	0.8	100	6.7	0.65	$20 \pm 3$
	4.7	1.0	100	3.6	0.65	$12 \pm 2$
	5.5	1.4	100	7.6	0.65	$21 \pm 3$
	5.9	1.8	100	13	0.65	$33 \pm 4$
Sm Mica	0.34	0.8	100	1.4	0.69	$58 \pm 9$
	0.30	1.0	100	0.60	0.69	$29 \pm 4$
	0.60	1.4	100	1.9	0.69	$45 \pm 7$
	0.60	1.8	100	1.7	0.69	$40 \pm 6$
Ta Makrofol	14	0.8	28.4	6.5	0.41	$40 \pm 8$
	14	1.0	29.6	15	0.41	$(9 \pm 2) \times 10$
	14	1.4	30.0	10	0.41	$(6 \pm 1) \times 10$
	14	1.8	30.0	15	0.41	$(9 \pm 2) \times 10$

Table 2 - Mean photofission cross section and fissility in the energy range 0.8-1.8 GeV.

Target nucleus (*)	Detector	$Z^2/A$	Mean photofission cross section, $\bar{\sigma}$ [ $\mu\text{b}$ ]	Mean nuclear fissility, $\bar{f}$
Al	CR-39	6.3	$(6 \pm 2) \times 10^2$	$(1.2 \pm 0.4) \times 10^{-1}$
Ti	CR-39	10.1	$(8 \pm 3) \times 10^2$	$(9 \pm 3) \times 10^{-2}$
Co	Makrofol	12.4	$34 \pm 7$	$(3.2 \pm 0.6) \times 10^{-3}$
Zr	Makrofol	17.5	$7 \pm 4$	$(4 \pm 2) \times 10^{-4}$
Nb	Makrofol	18.1	$6 \pm 4$	$(4 \pm 2) \times 10^{-4}$
Ag	Makrofol	20.5	$12 \pm 4$	$(6 \pm 2) \times 10^{-4}$
In	Makrofol	20.9	$38 \pm 9$	$(1.8 \pm 0.4) \times 10^{-3}$
Nd	Makrofol	25.0	$9 \pm 3$	$(3 \pm 1) \times 10^{-4}$
	Mica		$37 \pm 8$	$(1.4 \pm 0.3) \times 10^{-3}$
Sm	Mica	25.6	$(2 \pm 1) \times 10$	$(7 \pm 4) \times 10^{-4}$
Ta	Makrofol	29.5	$(6 \pm 3) \times 10$	$(1.8 \pm 0.9) \times 10^{-3}$

(\*) Isotopic abundances of the elements listed are those of the naturally occurring isotopes.



References

- (1) T. METHASIRI, S.A.E. JOHANSSON: Nucl. Phys. A167, 97(1971).
- (2) V.I. KASILOV, A.V. MITROFANOVA, YU. N. RANYUK, P.V. SOROKIN: Hochenergie und Atomkernphysik, Bd. 6(8), 1973.
- (3) V. EMMA, S. LO NIGRO, C. MILONE: Nucl. Phys. A257, 438(1976).
- (4) F.M. KIELY, B.D. PATE, F. HANNAPE, J. PETER: Z. Phys. A279, 331 (1976).
- (5) A.V. GANN, T.S. NAZAROVA, V.I. NOGA, YU. N. RANYUK, P.V. SOROKIN, YU. N. TELEGIN: Sov. J. Nucl. Phys. 30, 453 (1979).
- (6) J.D. PINHEIRO FILHO: Doctoral Thesis, Centro Brasileiro de Pesquisas Físicas-CBPF/CNPq, Rio de Janeiro-RJ (Brasil), December 1983.
- (7) J.R. NIX, E. SASSI: Nucl. Phys. 81, 61 (1966).
- (8) A.S. IL'INOV, E.A. CHEREPANOV, S.E. CHIGRINOV: Sov. J. Nucl. Phys. 32, 166 (1980).
- (9) W.D. MYERS: Droplet Model of Atomic Nuclei (Plenum, N.York, 1977).
- (10) R.L. FLEISCHER, P.B. PRICE, R.M. WALKER: Nuclear Tracks in Solids: Principles and Applications (University of California Press, 1975).
- (11) S.A. DURRANI, R.K. BULL: Solid State Nuclear Track Detection (Pergamon Press, Oxford, 1987).
- (12) D.A. DE LIMA, D. HUSMANN, J.B. MARTINS, O.A.P. TAVARES: Proc. Int. Conf. on Nuclear Physics, Florence (Italy), Aug. 29-Sept. 03, 1983, Contribution C35, vol. 1, pg. 353.
- (13) D.A. DE LIMA, J.B. MARTINS, O.A.P. TAVARES, D. HUSMANN, Proc. 6th Reunião de Trabalho sobre Física Nuclear no Brasil, Itatiaia-RJ, Brasil, 03-07 September, Contribution E-17(1983), pg. 27.
- (14) D.A. DE LIMA, J.B. MARTINS, O.A.P. TAVARES: Nucl. Instr. Meth. in Phys. Res. B30, 67 (1988).

- (15) V.S. BARASHENKOV, F.G. GEREGHI, A.S. ILJINOV, G.G. JONSSON, V.D. TONEEV: Nucl. Phys. A231, 462 (1974).
- (16) H.H. ANDERSEN and J.F. ZIEGLER: Hydrogen Stopping Powers and Ranges in All Elements (Pergamon Press, N.York, 1977).
- (17) M. DAMASHEK, F.J. GILMAN: Phys. Rev. D 1, 1319 (1970).
- (18) S.J. BRODSKY, J. PUPLIN: Phys. Rev. 182, 1794 (1969).
- (19) D.O. CALDWELL, V.B. ELINGS, W.P. HESSE, G.E. JAHN, R.J. MORRISON, F.V. MURPHY, D.E. YOUNT: Phys. Rev. Letters 23, 1256 (1969).
- (20) G.A. VARTAPETYAN, N.A. DEMEKHINA, V.I. KASILOV, YU. N. RANYUK, P.V. SOROKIN, A.G. KHUDAVERDYAN: Sov. J. Nucl. Phys. 14, 37 (1972).
- (21) I. KROON, B. FORKMAN: Nucl. Phys. A197, 81 (1972).
- (22) H.G. DE CARVALHO, J.B. MARTINS, O.A.P. TAVARES, V. DI NAPOLI, M.L. TERRANOVA, K. TESCH: Lettere Nuovo Cimento 14, 615 (1975).
- (23) A.V. MITROFANOVA, YU. N. RANYUK, P.V. SOROKIN: Sov. J. Nucl. Phys. 6, 512 (1968).